Modelling air flow and pollutant distribution inside street canyons with different roof shapes

Hui Wen[1] and Liora Malki-Epshtein[1]
[1]University College London, London, UK

ABSTRACT

This study uses Computational Fluid Dynamics (CFD) modelling to test the effect of roof shape on airflow and air pollution in and around street canyons. Street canyons are established as a primary factor in poor roadside air quality as they inhibit ventilation of the streets, and the importance of urban street canyon design in maintaining good air quality should not be underestimated (Moussiopoulos, 2003). The streets are modelled in ANSYS FLUENT, choosing a typical scaled-down street configuration found in several experimental studies (Meroney et al., 1996, Wen et al., 2013). The entire flow domain is simplified into a two-dimensional domain with six buildings to represent five continuous street canyons. The aspect ratio is fixed as 1.25, in which we expect a large vortex to form in the center of the street canyon (Karra, 2012). The roof shapes of these six buildings are set to various structures that are typically found in London. Compared to the well-studied simple case of symmetrical street canyons, where the buildings have continuous flat roofs and are modelled as simplified rectangular blocks, all other different roof shapes have resulted in different flow patterns and pollutant distributions within the street. These small-scale changes to roof pitch and size affect the shape of the vortex inside the canyon, and affect the overall ventilation of the street even under similar atmospheric flows. It is found that this can have a profound effect on the pollutant concentration field, with some cases leading to poor ventilation and reduced flushing of contaminants outwards of the street. The different roof shapes and geometries will be presented and their effect on pollution removal will be discussed.

INTRODUCTION

In street canyons, where tall buildings on both sides of a street block airflow and hinder ventilation, the environment inside and around the buildings can suffer from a build-up of heat and pollution, especially when the background atmospheric wind is perpendicular to the street (Li et al., 2006). The aspect ratio of the street, which is defined as the ratio of building height to street width, is the dominant factor determining overall flow patterns and pollutant distribution (Oke, 1988). Street canyons with low aspect ratio (building height to street width) are found to be helpful for pollutant removal, but in practice, urban street design is usually affected mainly by other factors such as land utilization. However, street features with scales smaller than building height and/or street width might have some notable impacts on both local flow field and pollutant dispersion (Huang et al., 2009). For example, geometric structures at roof level might have significant impacts on flow field and pollutant distribution because they affect the incoming flow before it reaches the bottom of the street canyon. Thus, for a street canyon with a given aspect ratio, finding favourable geometric structures that have a length-scale smaller than the building height can be a practical approach to alleviate the pollution build-up within the street. In this paper, we focus on the roof shape analysis through a Computational Fluid Dynamics (CFD) approach.

There are some precedents to the study of roof shape in street canyons. Rafailidis and Schatzmann (1996) carried out a series of wind tunnel experiments, in order to study the different impacts of wedge-shaped roof and flat-shaped roof on flow field and pollutant field. They found that a sloping roof confined within the urban canopy at the upstream building could reduce the street pollution levels in a wide street case. However, for a narrow street case, a sloping roof protruding above the urban canopy at the downstream building helped to reduce street pollution levels. Huang et al. (2009) did a similar study, but their study was based on CFD modelling approach. Their work reflected the great advantage of CFD over experimental work, in that complete flow-field information is available. They observed that the height of a wedge-shaped roof peak located upwind of a street canyon was a key factor to determine flow behaviours inside street canyons. Moreover, a wedge-shaped roof located upwind of a street canyon had more significant impacts than the roof at downstream location. Takano and Moonen (2013) found the critical roof slope of a wedge-shaped roof that would lead to a single vortex inside a street canyon breaking into two vortices. The latter flow pattern could result in a much higher concentration level on the ground due to limited mixing performance. They found the critical angle was around 18° in their case.

We carry out a study of some roof shapes that have not been considered before. We calculate the roof level pollutant flux and decompose the effects of advection and turbulent diffusion. These issues have not been considered in previous studies.

METHODOLOGY

Aimed to compare our model to previous experimental work Karra (2012) and modelling work Wen et al. (2013), we set the dimensions of flat buildings identical to the experimental work. The modelling work represents scaled-down experimental work conducted in a water channel. The street canyon distribution is shown in Figure 1. The buildings in the flat roof case are of dimensions 6cm×6cm, and the street widths are 4.8cm. This results in an aspect ratio 1.25. More information about the experimental settings can be found in Karra (2012). In all other cases with non-flat roofs, the peak of roof is kept as 6cm, while the height of eaves is 4.5cm. The third street canyon is chosen as the test street canyon, because the flow patterns inside the fourth and fifth street canyons maintain the same flow pattern as the third street canyon.

We carry out a two-dimensional model to reduce computational time compared to using a full three-dimensional model. We find that the convergence performance of the two-dimensional model is better than the extruded three-dimensional model. Eight typical shapes of roof are tested in this study, and they are shown in Figure 2. They are ①flat roof, ②terrace roof, ③leeward shed roof, ④windward shed roof, ⑤mansard roof, ⑥stepped roof, ⑦gabled roof and ⑧domed roof. It should be noted that they are regarded as general building structures at roof level rather than strict roof structures.

The modelling work is done on the commercial CFD software ANSYS FLUENT (ANSYS, 2009b). We apply RNG k-ε model as turbulence model with standard wall functions. This model was proposed and developed by Yakhot and co-works (Yakhot et al., 1992, Yakhot and Orszag, 1986). The model has a similar form as the standard k-ε model, but it has different model constants derived from RNG theory and an additional term in the dissipation equation. It is reported that this model yields better predictions than the standard k-ε model in backward facing step flow, buoyancy flow as well as street canyon flow (Chan et al., 2002, Chen, 1995, Yakhot et al., 1992). The model constants proposed by Yakhot et al. (1992) are used and listed in Table 1. The boundary settings are almost the same as previous work, and they are listed in Table 2. The distances before, after and above buildings are also implied in Table 2. The solution is obtained by SIMPLEC algorithm. The accuracy of advection term and other terms are selected as second-order accuracy. A 1×10^{-6} residual criterion is applied to all the equations. The total mesh number for each case is around 80,000, which is finer than our previous three-dimensional study Wen et al. (2013). More than 20 nodes are allocated along the street widths, and more than 30 nodes are set along the building heights.

The pollutant is modelled as passive scalar, which means the pollutant is advected by the flow but does not affect it. The source is placed on the ground of the middle of the third street canyon as a narrow area source. The width is set to 0.4mm which is 1/12 of the street width. The source is treated as an inlet boundary with a very small velocity to satisfy the required flux of pollutant through this narrow area source. Here, the velocity at the boundary is set to 5.61×10^{-5}m/s, and the passive scalar at the boundary is 0.023. We set the passive scalar to units g/L.

Table 1: Model constants of RNG k-ε model

C_μ	$C_{\varepsilon 1}$	$C_{\varepsilon 2}$	α_k	α_ε	η_0	β
0.0845	1.42	1.68	1.393	1.393	4.38	0.012

Table 2: Boundary conditions for this simulation

Position	Boundary	Explanation
Inlet	Velocity inlet	Using boundary profiles: $U=\frac{U_\tau}{\kappa}\ln\frac{y}{z_0}$ $k=\frac{{U_\tau}^2}{\sqrt{C_\mu}}\left(1-\frac{y}{0.2}\right)$ $\varepsilon=\frac{{U_\tau}^3}{\kappa(y+\delta_\nu)}$ With $U\tau=1.2\times10^{-2}$m/s, $\kappa=0.41$, $z_0=1.2\times10^{-4}$m, $\delta_v=1.1\times10^{-4}$m
Outlet	Outflow	10H after the last building, which is suitable for fully-developed flow
Top plane	Symmetry	Symmetry boundary as the most appropriate boundary in FLUENT, 2.3H above the building peaks①
Building surfaces	Wall	Smooth wall
Ground	Wall	Smooth wall
Source plane for emission	Inlet	Velocity 5.61×10^{-5}m/s with 0% turbulent intensity Passive scalar at inlet has a value 0.023

①This water depth is found to model the most accurately the conditions found in the experiment.

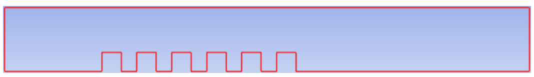

Figure 1: Building distribution and flow domain configuration (flow coming from left to right)

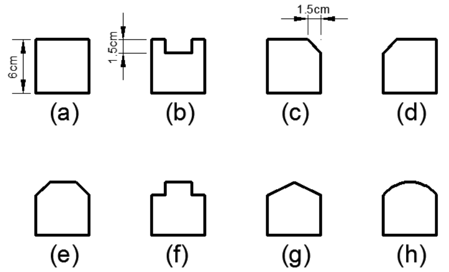

Figure 2: Eight roof shapes: (a)flat roof, (b)terrace roof, (c)leeward shed roof, (d)windward shed roof, (e)mansard roof, (f) stepped roof, (g)gabled roof and (h) domed roof

RESULTS

Five vertical lines are chosen inside the third street canyon. Their locations are in the middle of the third street canyon, 1.1cm left of the middle line, 2.2cm left of the middle, 1.1cm right of the middle line and 2.2cm right of the middle line. The velocity components along these five lines are displayed in Figure 3(a) to 3(e) respectively (flat roof case only). The green lines, red lines and blue lines correspond to the two-dimensional CFD results, the three-dimensional CFD results and the experimental measurement. Solid line represents horizontal velocity component, and dash lines represents vertical velocity component. These results will be compared in the next section to validate the viability of the two-dimensional model. The velocity magnitude contours for each case are given as Figure 4(a) to 4(h). The stream-lines are plotted in the same contour to display the flow pattern. The pollutant concentration contours are shown as Figure 5(a) to 5(h). The area-averaged pollutant levels below 4.5cm and 1.5cm are listed in Table 3. They are calculated by integration and then divided by the area (ANSYS, 2009a). A typical building height in the UK is around 10m. Therefore, the pollutant level below 1.5cm (1/4 of building peak) is a good representation of pollutant level close to the pedestrian level in the real world. The pollutant level below 4.5cm (3/4 of building peak) is an indication of the overall pollutant removal performance, as the street canyon structures below 4.5cm are the same in all the cases.

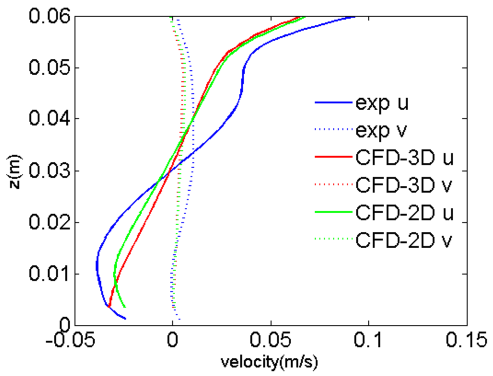

Figure 3(a): Velocity components along a vertical line; the line in the middle of the 3rd street canyon

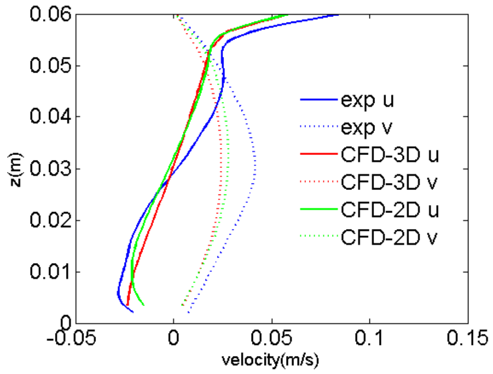

Figure 3(b): Velocity components along a vertical line; the line 1.1cm left of the middle line

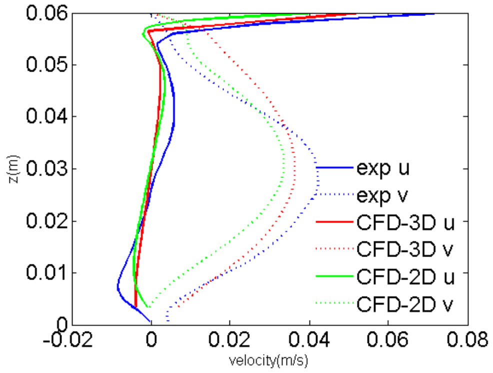

Figure 3(c): Velocity components along a vertical line; the line 2.2cm left of the middle line

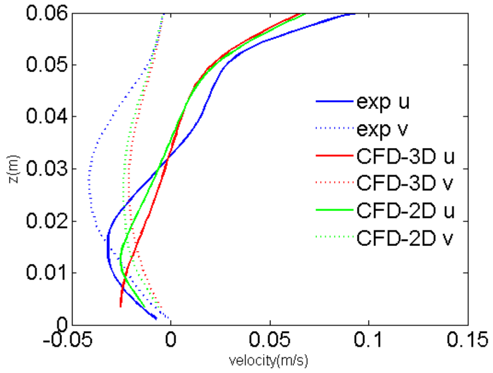

Figure 3(d): Velocity components along a vertical line; the line 1.1cm right of the middle line

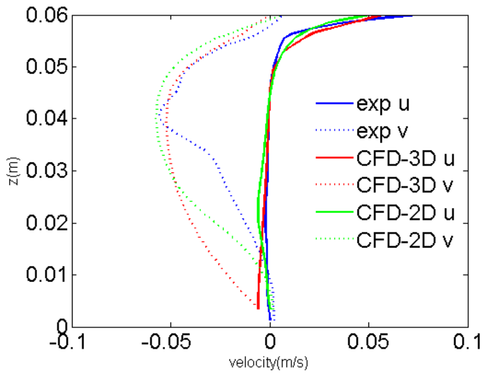

Figure 3(e): Velocity components along a vertical line; the line 2.2cm right of the middle line

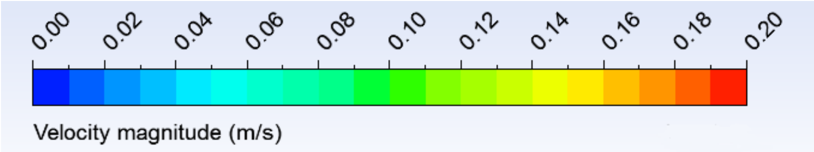

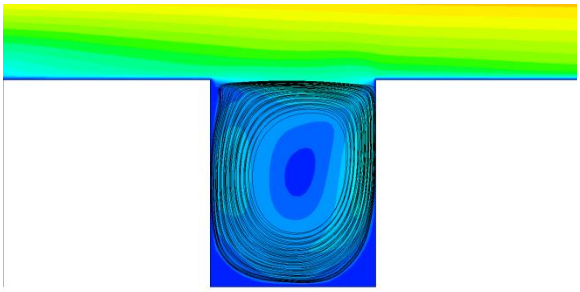

Figure 4(a): Velocity magnitude contour and velocity vector of flat roof case

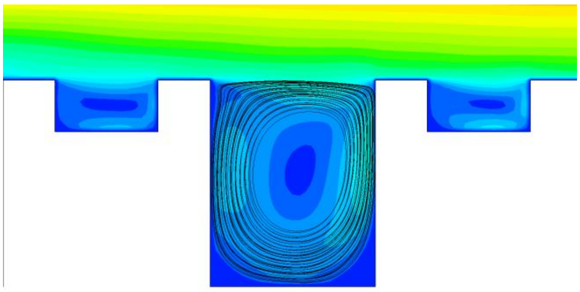

Figure 4(b): Velocity magnitude contour and velocity vector of terrace roof case

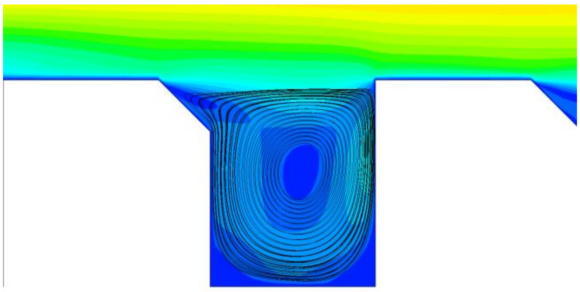

Figure 4(c): Velocity magnitude contour and velocity vector of leeward shed roof case

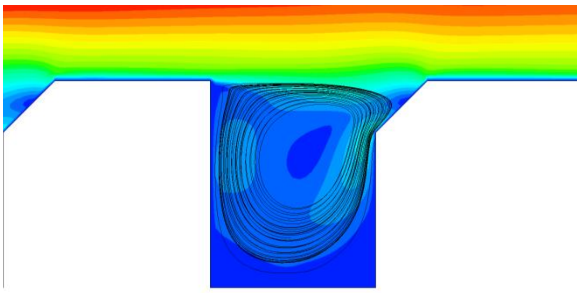

Figure 4(d): Velocity magnitude contour and velocity vector of windward shed roof case

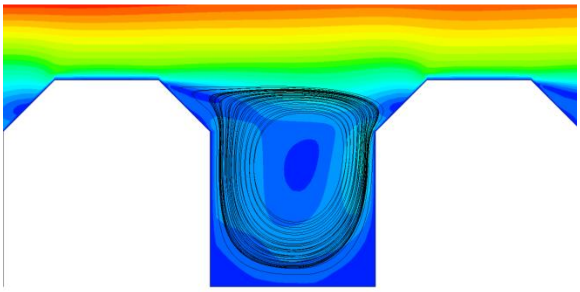

Figure 4(e): Velocity magnitude contour and velocity vector of mansard roof case

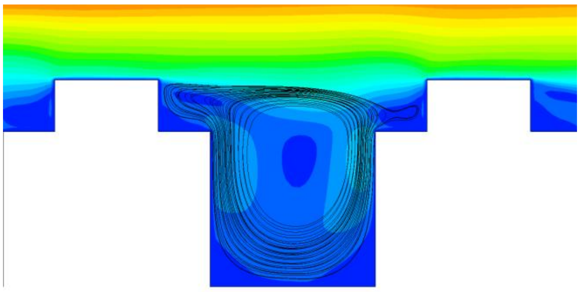

Figure 4(f): Velocity magnitude contour and velocity vector of stepped roof case

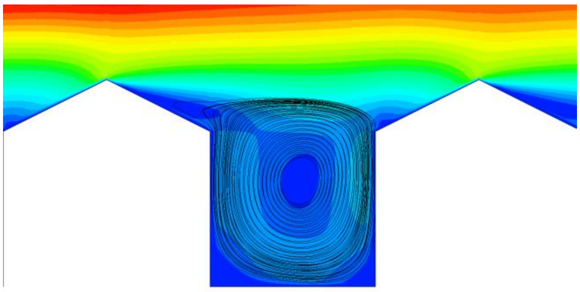

Figure 4(g): Velocity magnitude contour and velocity vector of gabled roof case

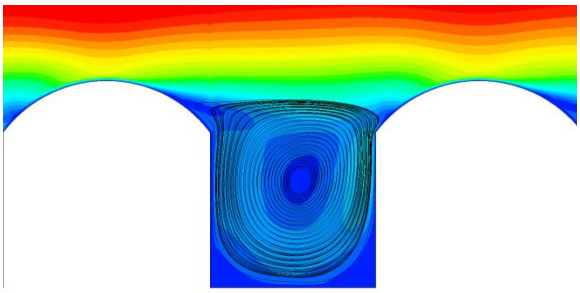

Figure 4(h): Velocity magnitude contour and velocity vector of domed roof case

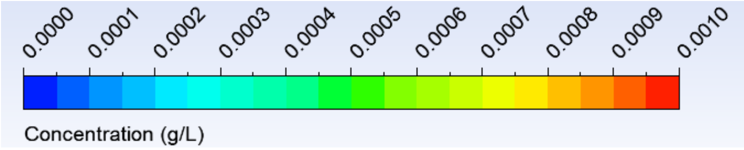

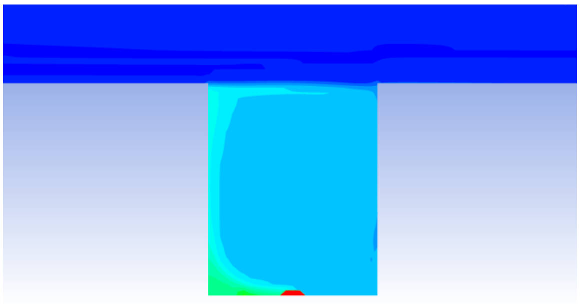

Figure 5(a): Pollutant concentration contour of flat roof case

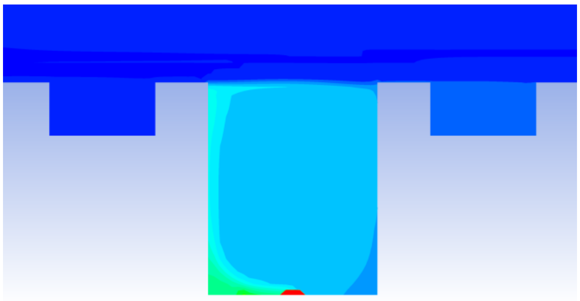

Figure 5(b): Pollutant concentration contour of terrace roof case

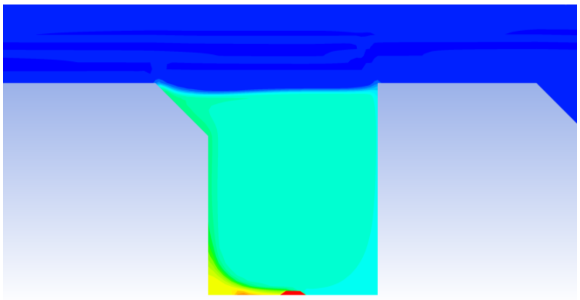

Figure 5(c): Pollutant concentration contour of leeward shed roof case

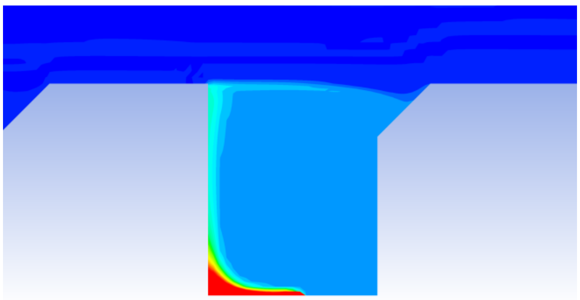

Figure 5(d): Pollutant concentration contour of windward shed roof case

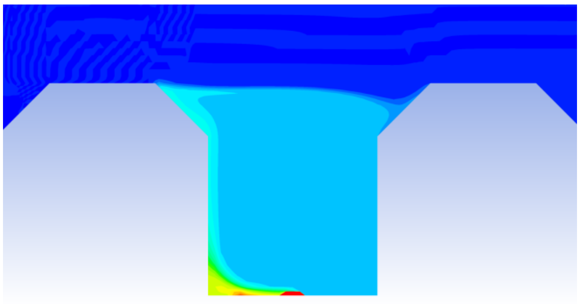

Figure 5(e): Pollutant concentration contour of mansard roof case

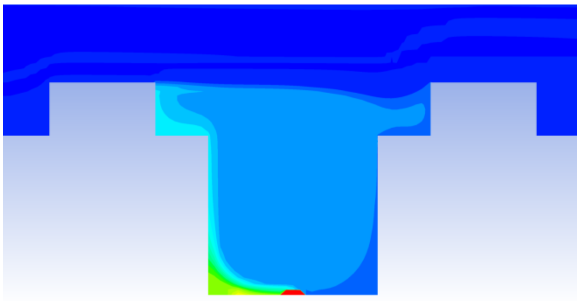

Figure 5(f): Pollutant concentration contour of stepped roof case

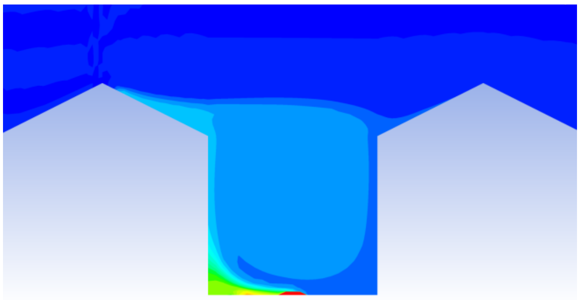

Figure 5(g): Pollutant concentration contour of gabled roof case

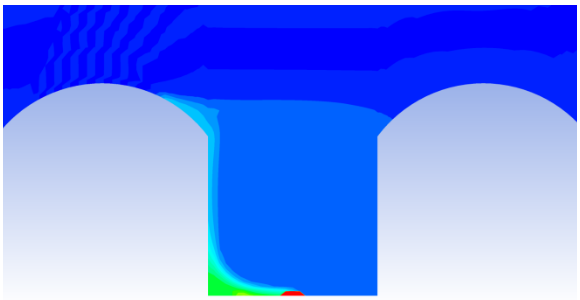

Figure 5(h): Pollutant concentration contour of domed case

Table 3: Concentrations below 0.45cm and 0.15cm

	flat	terrace	leeward shed	windward shed	mansard	stepped	gabled	domed
B45①	2.35	2.30	3.72	2.17	2.25	1.82	1.48	1.25
B15②	3.05	3.02	4.47	3.51	3.13	2.69	2.31	2.11

①Area-average concentration $\times10^{-4}$g/L, below the height 0.45cm

②Area-average concentration $\times10^{-4}$g/L, below the height 0.15cm

VALIDATION

The two-dimensional model is more practical for the study of several case studies and a finer mesh can be obtained, which is crucial for the quality of modelling of pollution concentrations. The accuracy of the two-dimensional model is close to that of our previous three-dimensional model for the flat roof case. According to Figure 3(a) to 3(e), the two-dimensional CFD results are very close to our previous three-dimensional results. In some locations, the two-dimensional results are even closer to the experimental measurements. For example, along the line 1.1cm to the right of the middle line, the vertical profile of the horizontal velocity component predicted by the two-dimensional model, which is shown in Figure 3(d), is closer to the experimental measurement. This is probably due to the mesh, which is twice as fine along the building facades and the street.

When the two-dimensional results are compared to the experimental measurements, we can find deviations in some locations. Those deviations (e.g. vertical components in Figure 3(d) and 3(e)) mostly occur in the positions close to wall. This is due to the limitation of using wall functions in CFD model. In the regions away from wall, we find absolute deviations are smaller, though the gradient of profile is a bit different from experimental measurement. In general, we could conclude this two-dimensional is qualitatively consistent with experimental work and have the same quality as previous three-dimensional CFD model.

DISCUSSION AND ANALYSIS

Flow pattern and velocity magnitude

In all cases, the general flow pattern is of one large clock-wise vortex formed inside the street canyon; while the size, shape and location of the vortex centre (indicated by the dark blue region in the middle) differ slightly between each case. Velocity magnitudes reach peak values near the windward side of the building.

However, some differences can be found in the velocity contour, and these differences are shown to have a significant influence on the pollutant distribution. Firstly, specific local flow features can be found near each type of roof. For example, recirculation can be seen near the roofs in all the non-flat roof cases. Furthermore, roofs with zero slope (flat roof and terrace roof) leads to higher velocity magnitudes inside the street canyon. This is reflected by a higher proportion of light blue region in their contours. Moreover, a much larger stagnation zone (indicated by dark blue colour) can be seen at the bottom in windward shed roof case. Finally, the transition region, which can be roughly considered as the region between the roof and the free-stream flow, varies a lot between cases, due to properties of the flow separation off the rooftops, at the edge of the leeward building. The region is larger in the cases of domed roof, windward shed roof, gabled roof, stepped roof and mansard roof, which presents with high velocities above the rooftops. This high velocity region is not found in the cases of leeward shed roof, flat roof and terrace roof.

Pollutant distribution

The pollutant information is shown in Table 3 and Figure 5(a) to 5(h). The area-averaged pollutant levels below height 4.5cm and 1.5cm are listed in Table 3, in order to indicate the overall pollutant level inside street canyon and the pollutant level near the pedestrian level. Here, we simply denote them as B45 concentration and B15 concentration. Leeward shed roof causes the highest B45 concentration and B15 concentration among all the cases. It leads to 58% B45 concentration and 47% B15 concentration higher than the flat roof case. Therefore, this design should be avoided. The second worst case is the windward shed case. Though its B45 concentration is not the second highest, extremely high levels of concentration (higher than 1×10^{-3}g/L, at least 40 times higher than the B45 concentration in windward shed roof case) are found near the ground, close to the leeward side building. Compared to the other cases, such high levels are only found around the emission source (indicated by red colour in contours). As a result, windward shed roof design could be a poor design in terms of pedestrian exposure to pollution.

The B45 concentration and the B15 concentration are quite similar between flat roof case, terrace roof case and mansard roof case. The B45 concentrations are around 2.3×10^{-3}g/L, and the B15 concentrations are around 3.1×10^{-3}g/L. These two concentrations are not as high as the leeward shed roof case.

The concentrations in stepped roof case, gabled roof case and domed roof case are relatively low. The B45 concentration and B15 concentration could reach up to 47% and 31% reduction compared to flat roof case.

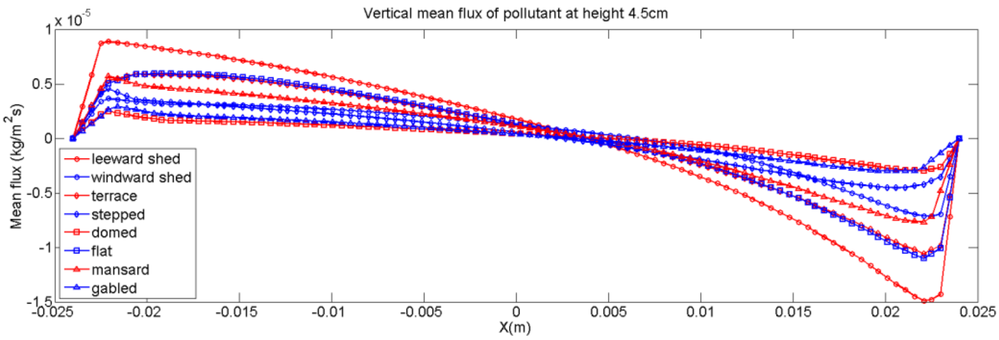

Figure 6(a): Vertical mean flux of pollutant at height 4.5cm

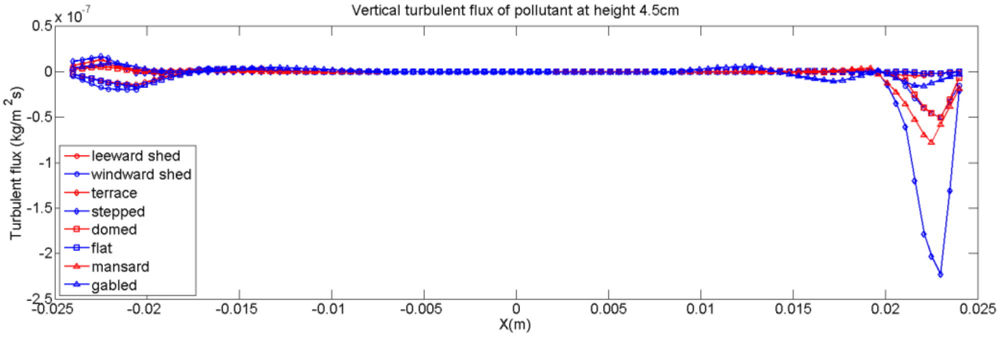

Figure 6(b): Vertical turbulent flux of pollutant at height 4.5cm

Table 4: Evaluation of roof designs according to the pollutant levels inside street canyon

Good design		Poor design
Stepped roof Gabled roof Domed roof	Flat roof Terrace roof Mansard roof	Windward shed roof Leeward shed roof

<u>Vertical mean flux and turbulent flux at roof level</u>

A horizontal line is drawn at height of 4.5cm in the third street canyon. Vertical mean flux of pollutant and vertical turbulent flux of pollutant are plotted along the line. They are calculated by the equations below, where v is vertical velocity component; y is vertical coordinate; Φ is passive scalar; Γ_{turb} is turbulent diffusion coefficient.

Vertical mean flux

$$mean\ flux = v\phi$$

Vertical turbulent flux

$$turbulent\ flux = \frac{\Gamma_{turb}}{\rho}\frac{\partial\phi}{\partial y}$$

The plots are given at Figure 6(a) and 6(b). A positive value indicates that the pollutant at a specific location is ventilated out of the street canyon through the vertical direction. It is noticed that the mean flux (y-axis scale) is two orders higher than the turbulent flux at the chosen height. Positive mean flux is found close to the leeward building, and negative mean flux is found close to the windward building. The neutral point (zero mean flux) is deviated to the windward building. The highest absolute flux happens in leeward shed roof case. In flat roof case and terrace roof case where the roofs do not have an inclined angle, the absolute mean flux is higher than the cases with an inclined angle (excluding leeward shed roof case). In stepped roof case, high negative turbulent pollutant occurs near the roof level of windward building, which indicates a steep negative concentration gradient there. However, this turbulent diffusion effect is still weaker than the advection effect which is negative as well.

<u>Comparison of different roof shapes</u>

The first finding is that the distortion of circular flow pattern inside street canyon highly changes the pollutant distribution. Windward shed roof case is the most typical example. Due to the existence of a shed on the windward building, the vortex is stretched towards that shed (see in Figure 4(d)). As a result, a much larger stagnation zone can be found at the bottom of the street canyon. A great deal of pollutant will accumulate in that region, and the overall pollutant level is also raised.

A low wind speed inside street canyon is not the only factor to lead to high pollutant levels. In the stepped roof case, the velocity magnitude at street level is significantly lower than in other cases. However, the pollutant level is lower than flat roof case, terrace roof case, leeward shed roof case and windward shed roof case. The reason for this seems to be the flow pattern demonstrated by the streamlines: pollution from the ground is effectively brought up to the rooftop through the vortex, and the distortion of the vortex at rooftop height allows better mixing with the boundary layer flow above the roofs, with pollutant flushing to the exterior.

The highest concentrations are found in the leeward shed roof case. In that case, a strong entrainment effect is found at the roof-level region close to the windward building. As indicated by Figure 6(a), the highest downward mean flux of pollutant represents that much more pollutant is brought back into the street canyon than any other cases. Velocities in the flow above the rooftops are lower and there appears to be less mixing between the in-street air and the layer above the roofs.

Gabled roof and domed roof are favourable designs for effective pollutant removal. The vortex size is smaller than for the other cases, and the vortex centre is lower down the street (see Figure 4(g) and 4(h)). It can be understood that the equivalent aspect ratio is lower than the aspect ratio based on building peak. The mansard roof and stepped roof have similar roof heights at roof edges, but neither case has a reduced vortex size. Therefore, the pollutant removal performance is not as effective as gabled roof case and domed roof case. This is probably because that the sharp roof at the leeward building in mansard roof case and stepped roof case leads to strong flow separation before the flow comes into the street. Therefore, a mild roof angle might be more conducive to pollutant removal.

CONCLUSION

In this paper, eight types of roof shape are modelled. Slight different flow patterns are found between each case. It is found that leeward shed roof is the worst design for pollutant removal. It leads to 58% B45 concentration and 47% B15 concentration higher than the flat roof case. Windward shed roof is the second worst design since a great amount of pollutants will be accumulated near the ground close to leeward building. Domed roof and gabled roof are favourable designs. They are 47% and 37% lower in B45 concentration and 31% and 24% lower in B15 concentration compared to the flat roof case. Although stepped roof case has relatively low velocity magnitude inside street canyon, the pollutant concentration does not show a higher level compared to the case with relatively high velocity magnitude.

REFERENCES

ANSYS, I. 2009a. ANSYS FLUENT 12.0 Theory Guide. U.S.A.: ANSYS, Inc.

ANSYS, I. 2009b. ANSYS FLUENT 12.0 User's Guide. U.S.A.: ANSYS, Inc.

CHAN, T. L., DONG, G., LEUNG, C. W., CHEUNG, C. S. & HUNG, W. T. 2002. Validation of a two-dimensional pollutant dispersion model in an isolated street canyon. *Atmospheric Environment,* 36**,** 861-872.

CHEN, Q. 1995. COMPARISON OF DIFFERENT k-ε MODELS FOR INDOOR AIR FLOW COMPUTATIONS. *Numerical Heat Transfer, Part B: Fundamentals,* 28**,** 353-369.

HUANG, Y., HU, X. & ZENG, N. 2009. Impact of wedge-shaped roofs on airflow and pollutant dispersion inside urban street canyons. *Building and Environment,* 44**,** 2335-2347.

KARRA, S. 2012. *An investigation of traffic related pollutants dispersion in heterogeneous street canyon.* Doctor of Philosophy, University College London.

LI, X.-X., LIU, C.-H., LEUNG, D. Y. C. & LAM, K. M. 2006. Recent progress in CFD modelling of wind field and pollutant transport in street canyons. *Atmospheric Environment,* 40**,** 5640-5658.

MERONEY, R. N., PAVAGEAU, M., RAFAILIDIS, S. & SCHATZMANN, M. 1996. Study of line source characteristics for 2-D physical modelling of pollutant dispersion in street canyons. *Journal of Wind Engineering and Industrial Aerodynamics,* 62**,** 37-56.

MOUSSIOPOULOS, N. 2003. *Air quality in cities,* Berlin, Springer.

OKE, T. R. 1988. Street design and urban canopy layer climate. *Energy and Buildings,* 11**,** 103-113.

RAFAILIDIS, S. & SCHATZMANN, M. 1996. Study on different roof geometries in a simplified urban environment.

TAKANO, Y. & MOONEN, P. 2013. On the influence of roof shape on flow and dispersion in an urban street canyon. *Journal of Wind Engineering and Industrial Aerodynamics,* 123, Part A**,** 107-120.

WEN, H., KARRA, S. & MALKI-EPSHTEIN, L. 2013. Modelling of street canyon geometries in CFD – A comparison with experimental results. *13th Conference of International Building Performance Simulation Association.* Chambery, France.

YAKHOT, V. & ORSZAG, S. A. 1986. Renormalization group analysis of turbulence. I. Basic theory. *Journal of Scientific Computing,* 1**,** 3-51.

YAKHOT, V., ORSZAG, S. A., THANGAM, S., GATSKI, T. B. & SPEZIALE, C. G. 1992. Development of turbulence models for shear flows by a double expansion technique. *Phys. Fluids,* 4**,** 1510-1520.